



HAL
open science

Optimization of polysaccharides extraction from a wild species of *Ornithogalum* combining ultrasound and maceration and their anti-oxidant properties

Mohammad Kazem Medlej, Batoul Cherri, Ghassan Nasser, François Zaviska, Akram Hijazi, Celine Pochat-Bohatier

► To cite this version:

Mohammad Kazem Medlej, Batoul Cherri, Ghassan Nasser, François Zaviska, Akram Hijazi, et al.. Optimization of polysaccharides extraction from a wild species of *Ornithogalum* combining ultrasound and maceration and their anti-oxidant properties. *International Journal of Biological Macromolecules*, 2020, 161, pp.958-968. 10.1016/j.ijbiomac.2020.06.021 . hal-03093126

HAL Id: hal-03093126

<https://hal.science/hal-03093126v1>

Submitted on 5 Jan 2021

HAL is a multi-disciplinary open access archive for the deposit and dissemination of scientific research documents, whether they are published or not. The documents may come from teaching and research institutions in France or abroad, or from public or private research centers.

L'archive ouverte pluridisciplinaire **HAL**, est destinée au dépôt et à la diffusion de documents scientifiques de niveau recherche, publiés ou non, émanant des établissements d'enseignement et de recherche français ou étrangers, des laboratoires publics ou privés.

Optimization of polysaccharides extraction from a wild species of *Ornithogalum* combining ultrasound and maceration and their anti-oxidant properties

Mohammad Kazem Medlej^{1,2}, Batoul Cherry^{1,2}, Ghassan Nasser², François Zaviska¹, Akram Hijazi², Suming Li¹, Céline Pochat-Bohatier¹

¹ Institut Européen des Membranes, IEM UMR 5635, Univ Montpellier, CNRS, ENSCM, Montpellier, France.

² Platform for Research and Analysis in Environmental Sciences (PRASE), Lebanese University, Beirut, Lebanon.

Corresponding Author email: Celine.Pochat@umontpellier.fr

See DOI:

Abstract:

Polysaccharides were extracted from a wild species of *Ornithogalum* by using three methods: maceration, ultrasound-assisted extraction, and combination of maceration and ultrasound. Extraction conditions were optimized by using response surface method (RSM) with a central composite design (CCD). Four parameters were considered in the optimization method, *i.e.* total extraction time, extraction temperature, ratio of water volume to raw material mass, and time percentage of ultrasound treatment in the extraction process. The optimal extraction yield was 81.7 %, 82.5 % and 85.7%, and the optimal polysaccharides yield was 74.7 %, 75.7 %, and 82.8% under the optimum conditions of maceration, ultrasound-assisted extraction and combined extraction, respectively. These results indicate that the combination method significantly improves the extraction and polysaccharides yields compared to traditional extraction methods. The combination method also allows reducing the time of ultrasound treatment and thus its adverse effects on polysaccharides. In addition, these results well corroborate with the theoretically predicted values. The NMR (¹H, ¹³C, HSQC, HMBC, and COSY) analysis shows that the extract is composed of fructo-polysaccharides with a backbone of (2→6)-linked β-d-fructofuranosyl (Fruf) and (2→1)-linked β-d-Fruf branched chains, and terminated with glucose and Fructose residues. The antioxidant activities of the extract were evaluated from ABTS radical scavenging activity, total antioxidant capacity, metal-chelating power and β-carotene bleaching test. Data show that the extract presents outstanding antioxidant activities.

Keywords: Ultrasonic-assisted extraction; optimization; polysaccharides; anti-oxidant activity.

1. Introduction

Synthetic antioxidant compounds such as butylated hydroxyanisole (BHA) are extensively employed as preservatives in pharmaceuticals, cosmetic and food industry. However, some studies have shown that BHA causes adverse effects on cells [1], and thus could have negative

39 impact on human health. Therefore, naturally occurring antioxidants have been attracting
40 more and more interest as they actually represent an alternative to synthetic ones.

41
42 More than 90% of the carbohydrate mass in nature is in the form of polysaccharides. Many
43 studies reported that various polysaccharides present remarkable antioxidant activities, and
44 could be used as healthy food additives [2]. *Ornithogalum* is a genus of perennial plants with
45 various species, including *Ornithogalum arabicum*, *saundersiae*, *caudatum Ait*, *dubium*, *nutans*,
46 *pyrenaicum*, *thyrsoides* and *umbellatum*. Polysaccharides extracted from *Ornithogalum*
47 *caudatum Ait* present outstanding antioxidant, anticancer, antimicrobial and anti-
48 inflammatory activities [3]. They have been used for the treatment of hepatitis, parotitis, and
49 cancers [3]. *Ornithogalum billardieri* is a non-edible wild plant widespread in Lebanon which
50 could be a potential source of valuable polysaccharides with promising bioactive properties. To
51 the best of our knowledge, this plant has never been studied, so far.

52 The extraction of polysaccharides represents an important issue for their applications in
53 pharmaceutical and agri-food industries [4]. Maceration is the most commonly used method
54 to extract polysaccharides due to its simplicity. Nevertheless, the major inconvenience of
55 maceration is the low extraction yield [5], long extraction time, and large energy consumption.
56 Ultrasound (US) treatment is a time and energy saving method which is widely used for
57 extraction of various polysaccharides [6]. It allows to reduce the particle size, to disrupt the cell
58 wall, and to improve the mass transfer from solid to liquid phase due to the intense shear
59 forces, thus leading to higher extraction yield [7]. Compared to maceration, US treatment
60 presents many advantages such as reduced extraction time, lower temperature, and in some
61 cases less water consumption [8]. Importantly, US extraction allows to improve the purity of
62 extracted polysaccharides, and their antioxidant activity [9]. However, US treatment can
63 provoke chain cleavage and compositional changes of polysaccharides due to the cavitation
64 effects [9]. Side reactions could also happen and lead to the formation of carbonyl and hydroxyl
65 radical groups.

66
67 The aim of this work was to implement and optimize a new extraction process combining both
68 US and maceration in order to improve the extraction yield while reducing the adverse effect
69 of US treatment. Different combinations of maceration and US treatment were tested to
70 extract polysaccharides from *Ornithogallum billardieri* using the Surface Response
71 Methodology (RSM) applied to an experimental model such as Box-Behnken design (BBD) and
72 central composite design (CCD) [10]. The studied operating parameters include the total
73 duration of the extraction process (time), the extraction temperature, the ratio of added water

74 volume to raw material mass, and the time ratio of US treatment in the total process (% US).
75 The extracted polysaccharides were characterized by using ^1H , ^{13}C , HSQC, HMBC, and COSY
76 NMR analysis.

77

78 The antioxidant properties of the polysaccharides extracted under optimal conditions were
79 investigated, including ABTS radical scavenging activity, total antioxidant capacity (TCA), metal-
80 chelating power, and β -carotene bleaching test so as to evaluate their potential for applications
81 in the agro-food industry as alternative to synthetic antioxidants.

82

83 **2. Experimental**

84 **2.1. Materials and reagents**

85 The onion plant *Ornithogalum* was collected in the region of Bekaa in Lebanon. The plant was
86 carefully washed, cut into small pieces, and freeze dried. The dried plant was manually crushed,
87 and sieved at 0.6 mm to obtain a homogeneous powder. Sulfuric acid, phenol, 2,2-azino-bis (3-
88 ethylbenzothiazoline-6-sulfonic acid) (ABTS), ascorbic acid, potassium peroxydisulfate, sodium
89 phosphate, ammonium molybdate, α -tocopherol, iron dichloride, ferrozine, diethylenediamine
90 (EDTA), phenol, anhydrous ethanol, butanol, and chloroform of analytical grade were
91 purchased from Sigma Aldrich, and used as received.

92

93 **2.2. Extraction of polysaccharides**

94 Before extraction, the powder was purified at 70°C using a Soxhlet for 2 days with ethanol as
95 solvent. This preliminary step allowed to eliminate all pigments, polyphenols, oligosaccharides,
96 simple oses and amino acids, and also to inactivate enzymes. The powder recovered from the
97 Soxhlet cartridge was vacuum dried overnight at 40°C, and then crushed and sieved at 0.6 mm.
98 The powder was added in ultrapure water, and homogenized for 30 sec at 3500 rpm in a Speed
99 mixer (Hauschild DAC 150.1 FVZ-K). Extraction then proceeded at a given temperature (25-
100 65°C) for predetermined time periods (10-60 min). The extraction temperature was controlled
101 ($\pm 0.2^\circ\text{C}$) using a thermo-cryostat (Vacuo-Temp P, Selecta) and a thermostat cell. The ratio of
102 the water volume to the powder mass varied in the range of 10 to 40 mL/g. Ultrasound
103 treatment was performed at fixed frequency (35 KHz) and power (120 W). The time ratio of
104 ultrasound treatment in the total extraction process (%US) varied between 0% and 100%. After
105 extraction, the aqueous solution was immediately centrifuged at 6000 rpm for 15 min three
106 times. The supernatant was lyophilized using a freeze-dryer (Freezone 4.5 Labconco). Finally,
107 the obtained powder was washed with ethanol, and vacuum dried up to constant weight.

108 The extraction yield (%) was calculated using Eq. 1.

109

110 Extraction yield (%) = [(Weight of dried product / Weight of crude powder)] × 100(Eq. 1)

111

112 **2.3. Total carbohydrates content**

113 The total carbohydrate content (TCC), also known as the polysaccharides yield, was determined
114 according to Dubois method [11]. The method allows to quantify all carbohydrate species,
115 including mono-, di-, oligosaccharides, their methyl derivatives and polysaccharides. A
116 calibration curve was first established from standard glucose solutions at concentrations from
117 0 to 100 µg/mL. 1 mL of standard solution was added to 5 mL of concentrated sulfuric acid,
118 followed by addition of 1 mL of 5% (v/v) phenol solution. After 10 min stirring at 100 °C, the
119 solution was cooled down to room temperature away from light. Finally, the absorbance was
120 measured using a spectrophotometer at 490 nm (λ max). The absorbance was then plotted
121 against glucose concentration to obtain a calibration curve. The samples are analyzed using the
122 same procedure to obtain the concentration of polysaccharides in samples. The total
123 carbohydrate content (%) of samples is determined using the following equation:

124

125 Total carbohydrate content (%) = [(Weight of polysaccharides / Weight of sample)] × 100
126 (Eq. 2)

127

128 **2.4. Extraction optimization**

129 **2.4.1 Single-factor experiments**

130 A series of preliminary experiments were first performed in order to determine the intervals of
131 the 4 parameters (time, temperature, volume to mass ratio, and US%), and the range of
132 extraction yield and polysaccharides yield. For each experiment, a single parameter was varied
133 while keeping the others constant: the time was varied from 10 to 60 min, the temperature
134 from 20°C to 80°C, the volume to mass ratio from 10 to 50 mL/g, and the US% from 0 to 100%.
135 The results obtained from single factor analysis were used to build a model based on RSM to
136 identify the interactions between parameters.

137

138 **2.4.2 Experimental design**

139 The Surface Response Methodology (RSM) is applied to the central composite design (CCD) for
140 the adaptation of a second order polynomial by the least square technique. Eq. 3 is used to
141 determine the effects of test variables to the searched responses (extraction yield and
142 polysaccharides yield) and the correlation between variables.

143

144

$$Y = \beta\kappa_0 + \sum_{i=1}^4 \beta\kappa_i X_i + \sum_{i=1}^4 \beta\kappa_{ii} X_i^2 + \sum_{i<j=2}^4 \beta\kappa_{ij} X_i X_j \quad (\text{Eq. 3})$$

145

146 Where Y is the predicted response, $\beta\kappa_0$ the intercept, and $\beta\kappa_i$, $\beta\kappa_{ii}$, and $\beta\kappa_{ij}$ the coefficients of
 147 linearity, quadratic and interaction, respectively. And X_i and X_j are the coded independent
 148 variables. The response function was also related to the coded variables (X_i , $i = 1, 2, 3$) and $i \neq j$,
 149 by a second-degree polynomial using the method of least squares.

150 The CCD consists of 2^n factorial points and 2^n axial points, with $n =$ number of factors studied
 151 and N_c central points (replicates in the center of the experimental domain). Four parameters
 152 have been taken into account in this study, i.e. Time X_1 (min), Temperature X_2 ($^{\circ}\text{C}$), Volume X_3
 153 (volume to mass ratio, mL/g), and US percentage X_4 (%). The CCD is thus composed by 16
 154 factorial points, 8 axial points and 5 central points, giving a total of 29 experiments. The axial
 155 points are placed at a distance $\alpha=2$ from the center, that makes the design rotatable. The range
 156 and levels of the variables are given in Table 1 according to the actual and coded values.

157 The regression coefficients of individual linear, quadratic and interaction terms were
 158 determined using Design-Expert (Version 11) software. They were then used to make statistical
 159 calculations, which generate dimensional and contour maps from the regression models.

160

161

Table 1 Independent variables and their levels used in the response surface design

Coded value	$\alpha = -2$	-1	0	+1	$\alpha = +2$
	Real Value				
Time (min)	10	22.5	35	47.5	60
Temperature ($^{\circ}\text{C}$)	25	35	45	55	65
Volume to mass ratio (mL/g)	10	20	30	40	50
% US (%)	0	25	50	75	100

162

163 2.5 Structural characterization

164 2.5.1 Fourier transform infrared (FT-IR)

165 FT-IR spectra were recorded using an IR-TF Nicolet IS50 Fourier counter exchange absorption
 166 infrared spectrometer (Bruker, Germany) over a range of 400–4000 cm^{-1} . The samples were
 167 analyzed as KBr pellets.

168

169 2.5.2 Size-exclusion chromatography (SEC)

170 Size-exclusion chromatography (SEC) was carried out using HPLC (DW-LC1620A) equipped with
 171 TSK gel PW5000 + PW3000 columns and refraction index and ultraviolet detectors. The
 172 temperature of the columns and detectors was 20 and 35 $^{\circ}\text{C}$, respectively. A pH 6 phosphate

173 buffer at 10 mg/mL was used as eluent at a flow rate of 1 mL/min. Calibration was realized
174 using pullulan standards with molar masses from 500 to 25000 Da. The results were processed
175 using OmniSEC software.

176

177 **2.5.3 NMR Spectroscopy**

178 ^1H , ^{13}C , HSQC, HMBC, and COSY NMR spectra were recorded using a Bruker Avance III
179 spectrometer operating at 600 MHz and 150 MHz, respectively. D_2O was used as solvent, and
180 the chemical shifts were expressed in ppm. The spectra were treated using Mestre Nova 12.0.0.
181 software package.

182

183 **2.6 Antioxidant activities**

184 *2.6.1. ABTS radical scavenging activity*

185 2,2-azino-bis (3-ethylbenzothiazoline-6-sulfonic acid) (ABTS^+) stock solution was prepared by
186 dissolving 7 mM ABTS with 2.45 mM $\text{K}_2\text{S}_2\text{O}_8$ in ultra-pure water, followed by stirring in the dark
187 for 12 h. The solution was diluted with ethanol to obtain an absorbance of $0.7 (\pm 0.02)$ at 734
188 nm at 30°C . 0.1 mL of sample at concentrations from 0.02 to 10 mg/mL was mixed with 3.9 mL
189 of the diluted solution of ABTS^+ . After 20 min incubation at 30°C , the absorbance was
190 measured at 734 nm. Ultrapure water was used as blank sample [12], and ascorbic acid as
191 positive control. The ABTS radical scavenging activity was calculated from the following
192 equation:

193

$$194 \quad \text{Scavenging rate (\%)} = [A_0 - (A_e - A_{ie})]/A_0 \times 100 \quad (\text{Eq. 4})$$

195

196 Where A_0 , A_{ie} and A_e are the absorbance of the blank sample, the positive control, and the
197 samples, respectively.

198

199 *2.6.2 Total antioxidant capacity (TCA)*

200 100 μL of samples at concentrations ranging from 0.025 to 10 mg/mL were mixed in a tube
201 with 1 mL of reagent (0.6 M sulfuric acid, 28 mM sodium phosphate and 4 mM ammonium
202 molybdate). The mixture was incubated at 95°C for 90 min. A phosphomolybdenum complex
203 was formed after cooling down to room temperature. Absorbance of the solution was
204 measured at 820 nm. Ultrapure water was used as control [13]. The antioxidant activity is
205 presented in terms of absorption.

206

207 *2.6.3. Metal-chelating power*

208 100 μ L of samples at concentrations ranging from 0.2 to 10 mg/mL were mixed with 50 μ L of
209 FeCl_2 (2 mM), and vigorously stirred for 5 min. Then 100 μ L of Ferrozine (5 mM) were added
210 together with 2.75 mL of ultrapure water. After 10 min at room temperature, the absorbance
211 at 562 nm was measured.

212 The blank sample was prepared without addition of ferrozine, while the negative control was
213 prepared without addition of test sample. Ethylenediaminetetraacetic acid (EDTA) was used as
214 positive control [14].

215 The antioxidant activity was calculated from the following equation:

216

$$217 \quad \text{Antioxidant activity \%} = [(A_{\text{control}} - A_{\text{sample}}) / A_{\text{control}}] \times 100 \quad (\text{Eq. 5})$$

218

219 Where A_{control} and A_{sample} are the absorbance of the negative control and the sample,
220 respectively.

221

222 2.6.4 β -carotene bleaching test

223 The inhibition of β -carotene bleaching was evaluated according to the method described by
224 Koleva *et al.* [15]. 0.5 mg of β -carotene was dissolved in a mixture of 1 mL of chloroform, 25 μ L
225 of linoleic acid and 200 μ L of Tween-80. The solvent was evaporated in a rotary evaporator at
226 45°C. 100 mL of ultrapure water was then added to the suspension under stirring. 2.5 mL of
227 freshly prepared suspension were transferred to a tube containing 0.5 mL of test samples at
228 concentrations from 0.05 to 5 mg/mL. The mixture is incubated for 2 h at 50 °C after
229 homogenization. Ultrapure water was used as control. Absorbance was then measured at a
230 wavelength of 470 nm. The antioxidant activity was calculated from the following equation:

231

$$232 \quad \text{Antioxidant activity (\%)} = [1 - (A_0 - A_{120})_{\text{test}} / (A_0 - A_{120})_{\text{control}}] \times 100 \quad (\text{Eq. 6})$$

233

234 Where A_0 and A_{120} are the absorbance of the sample or the control before and after 120 min
235 incubation.

236

237 2.7 Statistical analysis

238 The data processing is based on the statistical analysis performed by using the ANOVA Test
239 (Analysis of Variance). A value of $p < 0.05$ is considered statistically significant. The data are
240 expressed as mean \pm standard deviation (SD) for three replicates. The lack-of-fit test, F value,
241 determination of coefficient (R^2), adjusted determination coefficient (R_{adj}^2), coefficient of

242 variation (C.V.%) calculated from Design Expert were used to evaluate the adequacy of the
243 models.

244 **3 Results and discussion**

245 The challenge of this work is to find a compromise between the positive and negative effects
246 of US extraction and temperature on the extraction and polysaccharides yields, in order to
247 maximize the mass transfer without degrading the quality of the product of interest.

248 **3.1 Optimization of the extraction**

249 *3.1.1 Single-factor experiments*

250 Single-factor experiments were first performed to determine the effect of the 4 parameters,
251 i.e. extraction time, temperature, volume to mass ratio, and US %, on both of the total
252 extraction yield and polysaccharides yield. The results are presented in Fig. S1 (Supporting
253 information). The same trend is observed in all cases, i.e. an increase of the yields to reach a
254 maximum followed by a decrease.

255

256 Based on the results of single factor experiments, it appears that both the extraction and
257 polysaccharides yields are largely dependent on the extraction conditions, and the 4
258 parameters are inter-dependent. Opposite effects of the parameters are clearly evidenced. In
259 fact, hydrolysis of polysaccharides occurs under harsh conditions. It is thus essential to
260 understand the effect of each parameter on the extraction and polysaccharides yields and the
261 relationship between the parameters by applying the RSM, an efficient statistical technique for
262 optimizing complex processes. The following intervals are selected for the optimization study:
263 time from 22.5 to 47.5 min, temperature from 35 to 55°C, volume to mass ratio from 20 to 40
264 mL/g, and %US from 25 to 75%.

265

266 *3.1.2 RSM statistical analysis and models validity*

267 Based on the results obtained from single factor analysis, optimization was carried out by using
268 RSM to study the effect of four independent variables [X_1 : time, X_2 : temperature, X_3 : volume
269 (ratio of volume to mass), X_4 : %US]. The preliminary results pave the way to determine the
270 interactions between parameters and their influence on the investigated responses. Table 2
271 shows the matrix of variables in real values and the obtained responses. The predicted
272 response Y can be correlated to the variables by applying multiple regressions analysis method.
273 The fitting of response functions Y_1 (extraction yield) and Y_2 (polysaccharides yield) with the

274 experimental data gives a second-order polynomial equation. The analysis of variance table is
275 generated by the Design Expert software (Version 11) used in this study.

276 The extraction and polysaccharides yields obtained in the 29 experiments vary from 76.2 to
277 86.1% and from 70.1 to 82.9%, respectively. Such relatively high values in narrow ranges could
278 be explained by the fact that large amounts of polysaccharides can be easily extracted from the
279 superficial layer of the particles. However, harsher extraction conditions are required to extract
280 species located well inside the particles.

281
282

Table 2 RSM centrale composite design and results for extraction yield (Y_1) and polysaccharides yield (Y_2).

RUN	X_1	X_2	X_3	X_4	Y_1	Y_2
1	22.5	35	20	25	76.2	70.1
2	47.5	35	20	25	77.2	71.0
3	22.5	55	20	25	76.5	71.6
4	47.5	55	20	25	76.9	72.2
5	22.5	35	40	25	78.7	72.2
6	47.5	35	40	25	83.5	77.4
7	22.5	55	40	25	79.4	72.8
8	47.5	55	40	25	83.0	77.3
9	22.5	35	20	75	81.9	75.2
10	47.5	35	20	75	78.1	72.3
11	22.5	55	20	75	80.0	73.4
12	47.5	55	20	75	76.6	71.0
13	22.5	35	40	75	82.7	75.0
14	47.5	35	40	75	83.3	76.5
15	22.5	55	40	75	78.8	72.8
16	47.5	55	40	75	80.7	74.3
17	10	45	30	50	76.7	71.1
18	60	45	30	50	80.1	72.9
19	35	25	30	50	78.7	74.3
20	35	65	30	50	80.2	73.1
21	35	45	10	50	76.7	70.1
22	35	45	50	50	80.8	77.3
23	35	45	30	0	78.5	72.5
24	35	45	30	100	82.0	76.1
25	35	45	30	50	85.3	82.6
26	35	45	30	50	86.1	82.9
27	35	45	30	50	85.8	81.7
28	35	45	30	50	84.6	82.9
29	35	45	30	50	85.2	82.0

283
284 In order to highlight the significance of models, statistical indicators such Analysis of Variance
285 (ANOVA) and correlation coefficients (R^2 , adjusted R^2 and predicted R^2) are determined, as
286 shown in Table 3.

287 The ANOVA results show that both quadratic models developed for Y_1 and Y_2 are highly
288 significant with F values (Fisher coefficient) of 25.1 and 121.3, respectively. Considering also
289 the p-values well below 0.05 ($P < 0.0001$) and the negligible pure errors towards the quadratic
290 model, the lack of fit of these models is insignificant. The correlation coefficient R^2 , adjusted R^2
291 and predicted R^2 are 0.950, 0.912, and 0.780 for the extraction yield, and are 0.989, 0.981, and
292 0.959 for the polysaccharides yield, respectively. These values are reasonably close to 1,

293 showing a high degree of correlation. On the other hand, the Adeq. Precision is used to measure
 294 the signal to noise ratio, and a ratio above 4 is considered as acceptable. The obtained Adeq
 295 Precision is 15.5 and 32.3 for the extraction and polysaccharides yields, respectively, indicating
 296 a very high degree of precision and a good reliability of the experimental data. Further analysis
 297 of the statistical indicators in Table 3 also shows that the model developed for the
 298 polysaccharide yield presents slightly better precision than the one for the extraction yield.

299
 300

Table 3 Analysis of variance (ANOVA) for Response Surface Quadratic Model of extraction and polysaccharides yields

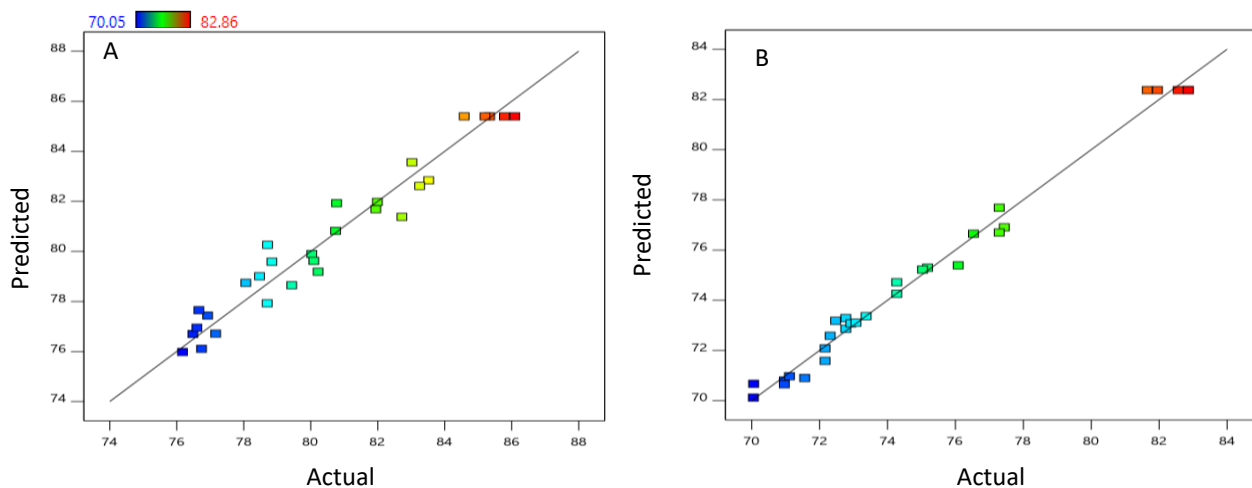
Source	Extraction yield					Polysaccharides yield				
	Sum of Squares	df	Mean Square	F Value	p-value	Sum of Squares	df	Mean Square	F Value	p-value
Model	263.55	12	21.96	25.13	< 0.0001	448.3	12	37.36	121.3	< 0.0001
Residual	13.99	16	0.87	-	-	4.93	16	0.31	-	-
Lack of Fit	12.65	12	1.05	3.15	0.1388	3.72	12	0.31	1.02	0.5444
Pure Error	1.34	4	0.33	-	-	1.21	4	0.3	-	-
C.V.%	1.16					0.74				

301

302 3.1.3 Regression equations and significant terms analysis

303 ANOVA tests are performed to evidence the significance of the studied parameters on the
 304 responses. The insignificant terms are removed in order to refine the developed models. As
 305 shown in Fig. 1, the experimental data are scattered around the theoretical line (Predicted vs
 306 Actual values), which indicates that the results obtained from the model well agree with the
 307 experimental data.

308
 309



310 **Fig. 1** Diagnostic plot (predicted vs actual values) for the adequacy of proposed model for extraction yield (A) and
 311 polysaccharides yield (B).
 312

313 The simplified equations for the extraction yield Y_1 and polysaccharides yield Y_2 are presented
 314 in terms of coded factor as follows:

315

316 $Y_1 = 85.40 + 0.49 X_1 - 0.27 X_2 + 1.46 X_3 + 0.74 X_4 + 1.04 X_1 X_3 - 0.92 X_1 X_4 - 0.63 X_2 X_4 - 0.56 X_3 X_4 - 1.69$
317 $X_1^2 - 1.42 X_2^2 - 1.60 X_3^2 - 1.23 X_4^2$ (Eq. 7)

318 $Y_2 = 82.38 + 0.53 X_1 - 0.29 X_2 + 1.51 X_3 + 0.55 X_4 + 1.04 X_1 X_3 - 0.85 X_1 X_4 - 0.68 X_2 X_4 - 0.51 X_3 X_4 -$
319 $2.59 X_1^2 - 2.17 X_2^2 - 2.17 X_3^2 - 2.02 X_4^2$ (Eq. 8)

320

321 The coefficients associated to the parameters or the interactions give a precise idea of how
322 they affect the corresponding responses (positively or negatively). Firstly, it appears that the
323 effect of the parameters and interactions follow the same trend for both Y_1 and Y_2 . Regarding
324 the coefficients, the ratio of volume to mass (X_3) is the most important factor affecting the
325 extraction process, followed by the US % (X_4) and the extraction time (X_1). The extraction
326 temperature (X_2) is the less significant parameter. It is well known that temperature generally
327 enhances the polysaccharide solubility and mass transfer, but it is also a destructive factor as
328 the US treatment. Raza *et al.* reported similar adverse effect of temperature [16]. Thus,
329 opposite effects could happen, minimizing the overall effect on the response. Regarding the
330 interactions, the most important one is referred to the synergistic (positive) effect between the
331 treatment time and the volume to mass ratio ($X_1 X_3$) which enhances the polysaccharide
332 extraction, in agreement with literature [16]. Indeed, both factors (X_1 and X_3) are non-
333 destructive parameters. When the ratio of volume to mass is higher, the overall driving force
334 is higher, thus accentuating the effect of the extraction time.

335 It is also noticed that US has systematically a negative effect when combined with another
336 factor. This means that US has a positive effect under mild extraction conditions, i.e. all other
337 parameters at low level. But as soon as the extraction conditions become harsher, the
338 destructive effect becomes predominant. This phenomenon is more accentuated with the
339 treatment time ($X_1 X_4$), which makes sense as US (percentage of X_1) is directly dependent on the
340 treatment time.

341

342 *3.1.4 Response surface analysis and optimization*

343 The two responses Y_1 and Y_2 follow the same trend as indicated above. Therefore, the same
344 effects and interactions of the parameters are expected for both responses. Only the
345 polysaccharides yield was investigated by using the Design-Expert to construct a three-
346 dimensional surface according to Eq. 8. The RSM was used to determine the relationship
347 between extraction parameters and responses, as shown in Fig. 2. Two variables are
348 continuously varied while keeping the two others constant.

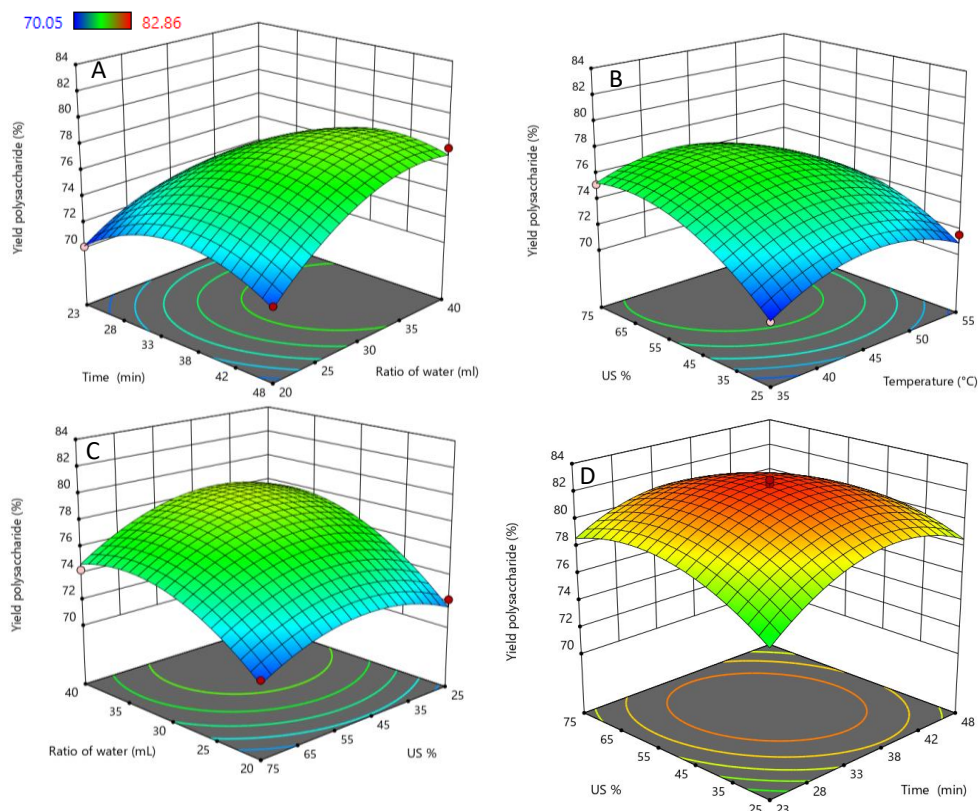
349

350 Fig. 2A presents the effect of interaction between volume to mass ratio and extraction time on
351 the polysaccharides yield, while the extraction temperature is fixed at 35°C and US% at 25%.
352 The highest polysaccharides yield of 78.2% is observed at 40 min and 36 mL/g. In fact, the
353 increase of volume to mass ratio results in increase of the polysaccharides yield. But in the
354 meantime, the extraction time required to obtain the maximum of polysaccharides increases
355 due to the dilution effect [17].

356
357 Fig. 2B presents the effect of temperature and US % while keeping the time fixed at 22.5 min
358 and volume to mass ratio at 20 mL/g. At low temperature (35°C), the polysaccharides yield
359 increases from 70.1 to 75.3% with US% increasing from 25 to 75. It appears that there is little
360 destructive effect of US under mild extraction conditions.

361
362 Fig. 2C presents the effect of volume to mass ratio and US% on polysaccharide yield at fixed
363 time (47.5 min) and temperature (55°C). Under these harsh conditions, the US treatment above
364 42% leads to a decrease by 8.2% of the maximum of polysaccharides yield.

365
366 Fig. 2D presents the effect of time and US% on polysaccharides yield while keeping the volume
367 to mass ratio at 30 mL/g and the temperature at 45°C (level 0). A remarkable increase of the
368 polysaccharides yield is detected with extraction time. However, an extraction time longer than
369 37.1 min leads to decrease of the polysaccharides yield. In fact, prolonged extraction time could
370 lead to cleavage of polysaccharide chains, resulting in decrease of the polysaccharides yield
371 [18]. The polysaccharides yield increases with the increase of US% up to a maximum at 51.7%.
372 Beyond, a decrease of the polysaccharides yield is observed. Additionally, the extraction time
373 required to obtain the maximum of polysaccharides yield becomes shorter with increase of
374 US%. These results evidence the effect of the main parameters and their interactions, which
375 allows to better understand the extraction process. In particular, it is clearly shown that the US
376 is definitely promoter of extraction because of improved mass transfer. But US also has a
377 destructive effect in combination with other parameters such as high extraction temperature.



379 **Fig. 2** 3D response surface plots showing the interactive effects of (A) time and volume to mass ratio at (-1, -1), (B)
 380 temperature and US% at (-1, -1), (C) volume to mass ratio and US % at (+1, +1), and (D) time and US % at (0, 0).

381

382 3.1.5 Validation of predictive models

383 The optimal extraction conditions to obtain the highest extraction and polysaccharides yields
 384 are given below: time (38.5, 37.1 min), temperature (43.5, 44.0°C), volume to mass ratio (35.4,
 385 33.8 ml/g), and US% (52.8, 51.7%). Under these conditions, the theoretical extraction and
 386 polysaccharides yields are 85.9% and 82.7% respectively.

387 Extraction was repeated three times under the optimal conditions in order to validate the two
 388 models for the extraction and polysaccharides yields. The obtained extraction yield is $85.7 \pm$
 389 0.2 %, and the polysaccharides yield is $82.8 \pm 0.1\%$. These values are very close to the
 390 theoretical ones, thus validating the models for evaluation of the effects of the 4 parameters
 391 on the extraction and polysaccharides yields.

392 In order to evidence the ambivalent effects of the US treatment, additional experiments were
 393 conducted at either 0% US (only maceration) or 100% US. The experimental results are then
 394 compared with the theoretical values obtained from the developed models, as shown in Table
 395 4. For the extraction yield, the first test was performed at 0% US under the predicted optimal
 396 conditions (time: 47.49 min; temperature: 47.84°C; volume to mass ratio: 40 mL/g), giving a
 397 maximum predicted extraction yield of 81.7%. The average extraction yield of three repeated
 398 experiments at 0% US was $81.7\% \pm 0.1\%$. The second test was performed at 100% US, which

399 allowed to obtain a maximum predicted extraction yield of 82.7% under the optimal conditions
400 (time: 30.03 min; temperature: 39.62°C; volume to mass ratio: 30.02 mL/g). The average
401 extraction yield of three repeated experiments at 100% US was 82.5% ± 0.1%.

402 In the case of the polysaccharides yield, at 0% US the maximum predicted polysaccharides yield
403 was 74.8% under the optimum conditions (time: 42.12 min; temperature: 47.1°C; volume to
404 mass ratio: 37.2 mL/g). The average yield of three repeated experiments was 74.7 ± 0.1%. At
405 100% US, the maximum predicted polysaccharides yield was 75.8% under the optimum
406 conditions (time: 32.41 min; temperature: 41.2°C; volume to mass ratio: 30.8 ml/g). The
407 average polysaccharides yield of three repeated experiments was 75.7 % ± 0.1%.

408 The model was then used to achieve the yield maximum under the mildest conditions. A
409 theoretical extraction yield of 83.0% was predicted with the following conditions: 23.7 min,
410 39°C, 22.6 mL/g and 69.5 % US. The experiences gave an average yield of 83.0 ± 0.1%, which is
411 nearly the same as the predicted value. This technique leads to significant decrease in time by
412 6.3 min, temperature by 0.7°C and volume to mass ratio by 7.4 mL/g, while a small increase in
413 extraction yield by 0.4% is obtained as compared to 100% US extraction (Table 4). Similarly, an
414 optimal polysaccharide yield of 76.3% is predicted under the following conditions: 23.1 min,
415 35°C, 21.3 mL/g and 65.3% US. Extraction performed three times under these conditions gave
416 a polysaccharide yield of 76.1% ± 0.1%. Comparison between the combined system and
417 extraction with 100% US indicates that the former allows a small increase in yield by 0.4%,
418 while decreasing significantly the time, temperature, and volume to mass ratio by 9.3 min,
419 6.2°C, and 9.5 mL/g, respectively (Table 4).

420 It is also of interest to compare the purity of the extract which is defined as the ratio of the
421 polysaccharides yield to the total extraction yield. Under the optimum conditions of
422 maceration, 100% US, and combined system, the purity of polysaccharides was 91.4 ± 0.1 %,
423 91.8 ± 0.2 %, and 96.6% ± 0.1%, respectively. Thus, the combination of maceration and US
424 allows improving the purity of the extract.

425 Chen *et al.* reported an optimized polysaccharide yield of 36.8 ± 1.8% for extraction from
426 *Ornithogalum Caudatum Ait* under the following conditions: frequency 40 kHz, temperature 60
427 °C, extraction time 60 min, ultrasound power 500 W, solvent to raw material 30 mL/g, 3 times
428 extraction [26]. The yields obtained in the present study (frequency 35 kHz, ultrasound power
429 120 W) are significantly higher, in agreement with successful optimization of ultrasound
430 assisted extraction. The combined extraction process allowed to reduce the sonication time,
431 and thus to prevent excessive polysaccharide degradation.

432

433
434

Table 4 Comparison of parameters, predicted and experimental values for optimization of extraction yield (Y1) and polysaccharides yield (Y2) by mixed system, maceration and US treatment

X ₁ (min)	X ₂ (°C)	X ₃ (mL/g)	X ₄ (%)	Predicted (%)	Experimental (%)
Y1					
38.5	43.5	35.3	52.8	85.9	85.7 ± 0.2%
47.5	47.8	40	0	81.7	81.7 ± 0.1%
30.0	39.6	30.0	100	82.6	82.5 ± 0.1%
23.7	38.9	22.6	69.5	83.0	83.0 ± 0.1%
Y2					
37.1	44.2	33.8	51.7	82.7	82.8 ± 0.1%
42.1	47.1	37.1	0	74.8	74.7 ± 0.1%
32.4	41.2	30.8	100	75.8	75.7 ± 0.1%
23.1	35	21.3	65.3	76.3	76.1 ± 0.1%

435

436 The extract with optimal purity of polysaccharides, namely OP%US, was obtained under the following conditions:
437 time 37.1 min, temperature 44.2°C, volume to mass ratio 33.8 mL/g, and US% 51.7%. OP%US was used for further
438 analyses.

439

440 **3.2 Structural characterization**

441 **3.2.1 FT-IR analysis**

442 The FT-IR spectrum of OP%US is presented in Fig. S2 (Supporting information). The large band
443 at 3405 cm⁻¹ is assigned to the stretching vibration of O–H groups, and the band at 2941 and
444 2896 cm⁻¹ were assigned to the stretching of –CH₃ and –CH₂ groups respectively. The band in
445 the range of 1420 cm⁻¹ belongs to the deformation vibration of C–H bond. The monosaccharide
446 of OP%US has pyranose rings as evidenced by two strong absorption bands of C–O–C
447 asymmetric stretching at 1132 cm⁻¹ and 1027 cm⁻¹. The band at 931.2 cm⁻¹ is attributed to the
448 symmetric stretching of furan rings. And the band detected at 599 cm⁻¹ is assigned to the
449 presence of the skeletal –CH₂ of pyranose rings. An α-configuration in the polysaccharide is
450 confirmed by the presence of characteristic absorptions at 818 cm⁻¹. Therefore, OP%US was an
451 α-configuration polysaccharide and consisted of pyranoside and funanside rings[19,20].

452

453 **3.2.2 Size-exclusion chromatography analysis**

454 From the results obtained in the RSM experiments, it appears that chain cleavage of
455 polysaccharides occurred to some extent during extraction. GPC analysis was then performed
456 for the corners of the design expert model in order to figure out the effect of extraction
457 parameters on the molar masses of the extracts, as summarized in Table 5. The effect of
458 extraction time is evidenced from the comparison between runs 17 and 18 since different
459 extraction times were used while keeping the three other parameters constant. Similarly, the
460 effect of extraction temperature and US % is evidenced from the comparison between runs 19
461 and 20, and runs 23 and 24, respectively.

462 In runs 17 and 18, the average molar mass (Mw) decreases from 5190 to 2940 Da when the
463 extraction time is raised from 10 to 60 min at fixed temperature (45°C), volume to mass ratio
464 (30 mL/g), and US% (50%). In the meantime, the dispersity ($\bar{D} = Mw/Mn$) slightly increases from
465 1.41 to 1.53. The negative effect of ultrasonic time on the molar mass of schizophyllan has been
466 also reported by Zhong *et al.* [21].

467 In runs 19 and 20, with the extraction temperature increasing from 25 to 65°C, the Mw of the
468 extract slightly decreases from 3180 to 2830 Da, whereas the dispersity remains almost
469 unchanged.

470 Finally, in runs 23 and 24, with increase of US treatment from 0% to 100%, the Mw slightly
471 decreases from 3350 to 3030 Da, and the dispersity remains almost unchanged. These results
472 suggest that long extraction time, high extraction temperature, and ultrasound treatment
473 provoke chain cleavage and molar mass decrease of the extract, which could affect the extract
474 yield as shown in the RSM experiments.

475
476

Table 5 Molar mass (Mw) and dispersity (\bar{D}) of the extract obtained in selected runs

Run	Time (min)	Temperature (°C)	% US (%)	Ratio (mL/g)	Mw (Da)	\bar{D}
17	10	45	50	30	5 190	1.41
18	60	45	50	30	2 940	1.53
19	35	25	50	30	3 180	1.49
20	35	65	50	30	2 830	1.52
23	35	45	0	30	3 350	1.50
24	35	45	100	30	3 030	1.52

477
478
479

3.2.3 NMR Spectroscopy

480 Various NMR analyses, including 1H , ^{13}C , HSQC, HMBC, and COSY NMR were performed to
481 determine the composition of the extract.

482

483 The ^{13}C NMR in Fig. 3A presents signals in the region of 59.0-61.48, 73.3-75.15, 57.3-77.77,
484 79.05-82.5, and 103.0-104.2 related to the C₁, C₆, C₄, C₃, C₅, and C₂ of fructose rings respectively.
485 Additionally, four anomeric C₂ carbon signals are detected (103.11, 103.76, 103.90, and 103.95
486 ppm), which indicates the presence of four fructose residues, *i.e.* β -d-Fruf-(2 \rightarrow , \rightarrow 1,6)- β -d-
487 Fruf-(2 \rightarrow , \rightarrow 1) β -d-Fruf-(2 \rightarrow , and \rightarrow 2) β -d-Fruf-(6 \rightarrow respectively respectively designated as
488 residues B, C, D, and E.

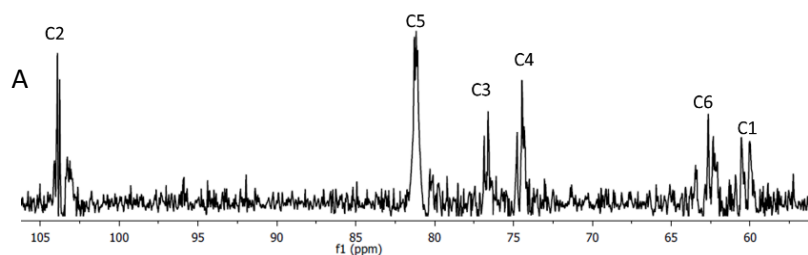
489

490 Fig. 3B presents the 1H NMR spectrum of the extract. Small signals are detected around 2.4, 2.5
491 and 2.7 ppm, which could be assigned to the presence of amino acids, carboxylic acids, alcohols
492 or phenols, in agreement with literature [22]. The signals at 3.8-3.7, 4.27, 4.13, 3.89, and 3.86-

493 3.68 ppm belong to the protons of fructose ring from H₁ to H₆, whereas the signals at 3.50,
494 3.59, and 3.98 ppm are attributed to the protons H₄, H₂ and H₅ of glucose, respectively. The
495 signal at 5.45 ppm indicates the presence of a proton on α of anomeric carbon. This proton
496 belongs to glucose named as residue A as fructo-ketose has no anomeric proton, which is in
497 agreement with FTIR results [23]. The chemical shifts for H₁, H₃, H₄ of residues B, C, D, and E of
498 fructose presented in Table 6 were determined from ¹H, HSQC, ¹H–¹H COSY spectra, and the
499 assignment of H₅ and H₆ realized from the ¹H–¹H COSY and HMBC spectra.

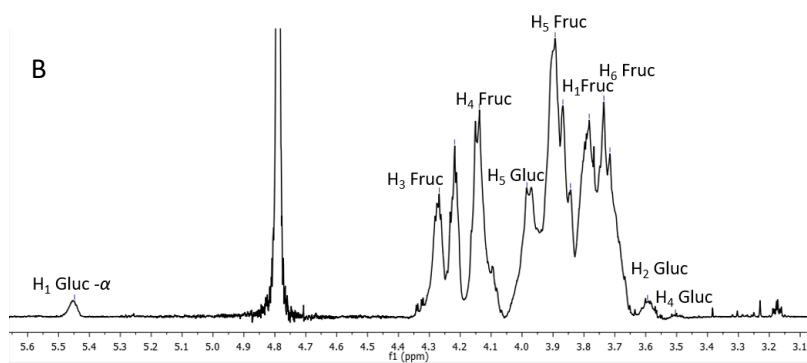
500
501 The HQSC spectrum fig. 3C of the extract presents typical signals at 81.08/3.9 and 80.28/3.98
502 ppm assigned to the C₅ of →2) β-d-Fru-(1→ and →2) β-d-Fru-(6→, respectively [24]. The
503 signals of H₁, H₃, H₄, H₅ and H₆ of fructose are related to the carbon signals at 60.46, 76.62,
504 74.46, 81.08, and 63.37 ppm, respectively. Meanwhile, the signals at 3.51, 3.59, 3.79, 3.98, 3.9-
505 3.7, and 5.45 ppm are linked to C₄ 69.32, C₂ 71.18, C₃ 72.52, C₅ 71.67, C₆ 61.9, and C₁ of anomeric
506 carbon 92.15 ppm for glucopyranose ring, respectively [25].

507
508 The sequence among residues and the linkage sites were achieved using the HMBC spectrum
509 which provides signals correlations between protons and carbons (Fig. 3D). The various signals
510 are assigned as follows. C₂ (103.11 ppm) for residue B and H₁ (3.91 ppm) for residue D
511 (BC₂/DH₁), suggesting that C₂ of residue B is linked to O-1 of residue D. Similarly, cross signals
512 at 103.11/3.89 ppm are assigned to BC₂/EH₆, 103.76/3.73 ppm to CC₂/CH₆, 103.93/3.71 ppm to
513 DC₂/CH₁, 103.93/3.91 ppm to DC₂/DH₁, 103.95/3.73 ppm to EC₂/CH₆, and 103.96/3.89 ppm to
514 EC₂/EH₆. Thus, the results obtained from HMBC suggest the following sequences: BC₂→ EO₆,
515 CC₂→ CO₆, DC₂→ CO₁, DC₂→ DO₁, EC₂→ CO₆, and EC₂→ EO₆. Finally, the COSY spectrum in Fig.
516 3S (Supporting information) shows cross signals between H₃/H₄; H₄/H₅ and H₅/H₆, in agreement
517 with literature [26].

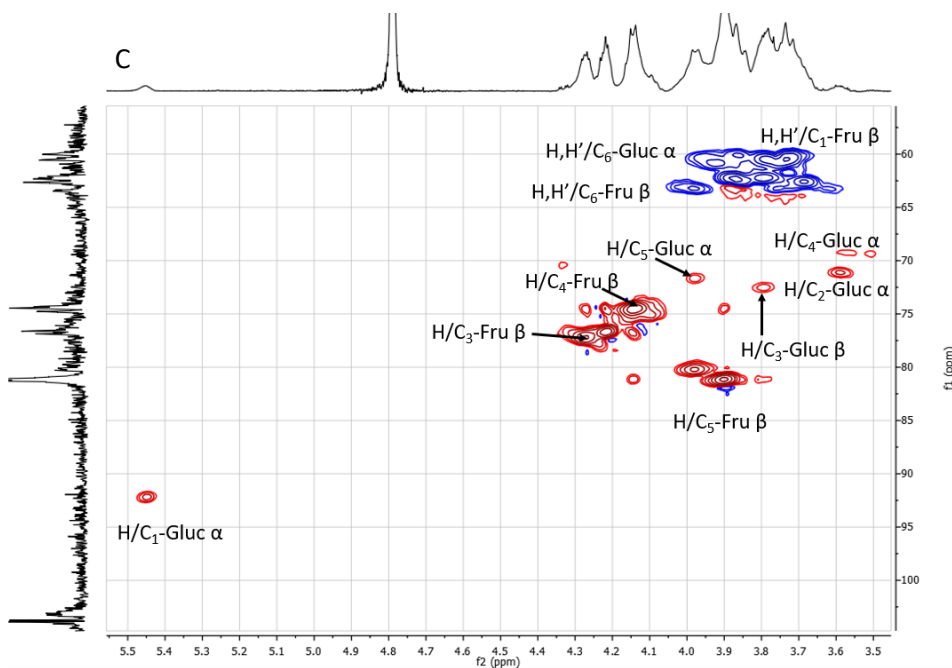


518

519
520



521



522

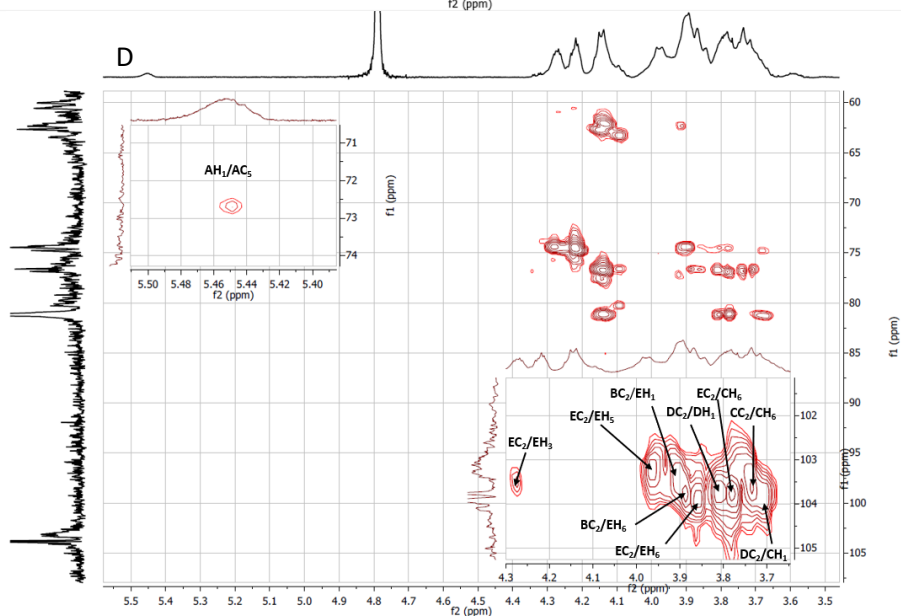


Fig. 3 ^1H (A), ^{13}C (B), HSQC (C), and HMBC(D) NMR spectra of OP%US, sample obtained with optimal purity of polysaccharides.

523
524
525
526

527
528
529

Table 6 ¹H and ¹³C NMR chemical shifts of OP%US

	C ₁ /H ₁	C ₂ /H ₂	C ₃ /H ₃	C ₄ /H ₄	C ₅ /H ₅	C ₆ /H ₆
-d-Glcp-(1 →residue A	92.15 / 5.45	71.18/3.59	72.52/3.79	69.32/3.51	71.67/3.98	61.9/3.74
β-d-Fruf-(2 →residue B	60.55/3.78	103. 11/-	76.57/4.28	74.42/ ^a 4.12	81.28/3.92	62.65/3.8
→1,6) β-d-Fruf-(2 →residue C	57.25/3.71	103.76/-	76.98/4.28 ^a	74.34/4.14	80.31/3.88	62.19/3.73
→1) β-d-Fruf-(2 →residue D	60.46/3.91	103.93/-	76.62/4.27	74.46/4.15 ^a	81.08/ 3.9	63.37/3.74
→2) β-d-Fruf-(6 →residue E	60.04/3.8	103.95/-	76.85/4.16 ^a	74.77/4.01	80.28/ 3.98	62.31/3.89

530 ^aUnresolved from other signals.

531
532
533

3.3 Antioxidant activity

534

535 3.3.1 ABTS radical scavenging activity

536 Fig. 4A presents the ABTS radical scavenging activity changes of OP%US as a function of
537 concentration, in comparison with ascorbic acid as a reference. The antioxidant activity of
538 OP%US increases with concentration to reach a maximum of 96.4% at 10 mg. The half maximal
539 inhibitory concentration (IC₅₀) is 1.28 ± 0.13 mg/mL. In the case of ascorbic acid, a very sharp
540 increase of the antioxidant activity is observed with concentration to reach 100% at 0.1 mg/mL.
541 Luo et al. reported a maximum scavenging activity of 28.0% and 82.6% for different fractions
542 of polysaccharides extracted from *Dendrobium nobile Lindl* against ABTS^{•+} at 2 mg/mL [27]. Hu
543 et al. studied the ABTS^{•+} scavenging activity of different fractions of polysaccharides extracted
544 from *Flammulina velutipes*. The maximum activity was 36.7%, 42.4%, and 61.8% at a
545 concentration of 3 mg/mL, with an IC₅₀ value of 2.8 mg/mL [28]. Comparison with literature
546 data suggests that OP%US has a good scavenging activity against ABTS^{•+}.

547
548

548 3.3.2 Total antioxidant capacity (TCA)

549 Mo (VI) is able to combine with proteins at the metal-binding site and to cause DNA and protein
550 damage [29], based on the reduction of Mo (VI) to Mo (V) by the formation phosphate/Mo (V)
551 complex at acidic pH. Fig. 4B presents absorbance changes of OP%US as a function of
552 concentration compared to BHA and α-tocopherol, two commonly used food additives. High
553 absorbance indicates high antioxidant activity. When the concentration increases from 0.025
554 to 5 mg/mL, the absorption increases from 0.14 to 2.04, from 0.02 to 0.9 and from 0.01 to 1.4
555 for α-tocopherol, BHA and OP%US respectively. It is noticed that the absorption of OP%US
556 becomes higher than that of BHA beyond 4 mg/mL. These results suggest that OP%US presents
557 a remarkable TCA capacity.

558
559

559 3.3.3 Metal-chelating power

560 The chelating agents are reported as secondary antioxidants because they can reduce the
561 redox potential, thereby stabilizing the oxidized form of the metal ion [30]. The ferrous
562 chelating capacity was evaluated from absorption measurement at 562 nm. Fig. 4C presents
563 the chelating capacity changes of OP%US as a function of concentration, using EDTA as a
564 reference. The chelating activity of OP%US gradually increases with increasing concentration,
565 reaching a maximum of 79.7 % at 10 mg/mL. The IC₅₀ of OP%US is 3.7 mg/mL. In contrast, the
566 chelating activity of EDTA rapidly increases with concentration to reach 100% at 0.4 mg/mL.
567 Nobre et al. investigated the chelating activity of various polysaccharides. The authors obtained
568 a maximum chelating activity of 69.9, 57.8, 46.1, and 43.3% for polysaccharides extract from *C.*
569 *Prolifera*, *C. Sertularioides*, *D. Cervicornis*, and *D. Mertensis* at 2 mg/ml, respectively [31]. Qi et
570 al. determined the chelating activity of sulfated polysaccharides extracted from *Ulva pertusa*.
571 Data show that the maximum activity is 36% and 10% for highly or less sulfated polysaccharides
572 at 2 mg/mL, respectively [32]. Comparison with literature data indicates that OP%US exhibits
573 an acceptable Fe²⁺ chelating activity.

574

575 3.3.4 *β*-carotene bleaching test

576 Linoleic acid generates peroxide radicals that will oxidize highly unsaturated *β*-carotene, known
577 as provitamin A which turns from red color to transparency. Antioxidant compounds are able
578 to neutralize free radicals, and thus preventing the oxidation and bleaching of *β*-carotene [33].
579 This test is of major importance for human safety as it allows to determine the ability of
580 samples to neutralize lipophilic free radicals that can easily enter human cells causing serious
581 damage to DNA [34]. Two other samples, namely OP M (only maceration) and OP 100%US (only
582 ultrasound), were prepared under the same conditions as OP%US but with or without
583 ultrasound.

584 Fig. 4D presents the *β*-carotene bleaching data of the three samples as a function of
585 concentration in comparison with BHA as reference. The results show that the antioxidant
586 activity of OP M, OP%US and OP 100%US are enhanced with increasing concentration from
587 0.05 to 5 mg/mL. A maximum capacity of 62.5% ,98.1%, and 82.8% are obtained at 5 mg/mL
588 for OP M, OP%US and OP 100%US, respectively. BHA exhibits slightly higher activity to *β*-
589 carotene bleaching than OP%US in the 0.05 to 0.5 mg/mL concentration range. No significant
590 difference is noticed between OP%US and BHA in the range from 1.0 to 5.0 mg/mL. The IC₅₀
591 of OP M, OP%US and OP 100%US are 0.82 ± 0.05, 0.131 ± 0.03 and 0.29 ± 0.03 mg/mL,
592 respectively. Chen et al.,Guo et al. and Shang et al. reported that ultrasound treatment
593 enhances the antioxidant activity [18][35]]. Tang et al. observed that the antioxidant activity of
594 polysaccharide from *Cyclocarya paliurus* slightly increases with US treatment from 55.5% and

595 59.0% at 500 µg/mL [36]. OP 100%US presents higher activity compared to OP M, whereas the
 596 combined system presents the highest activity compared to the traditional extraction systems.
 597

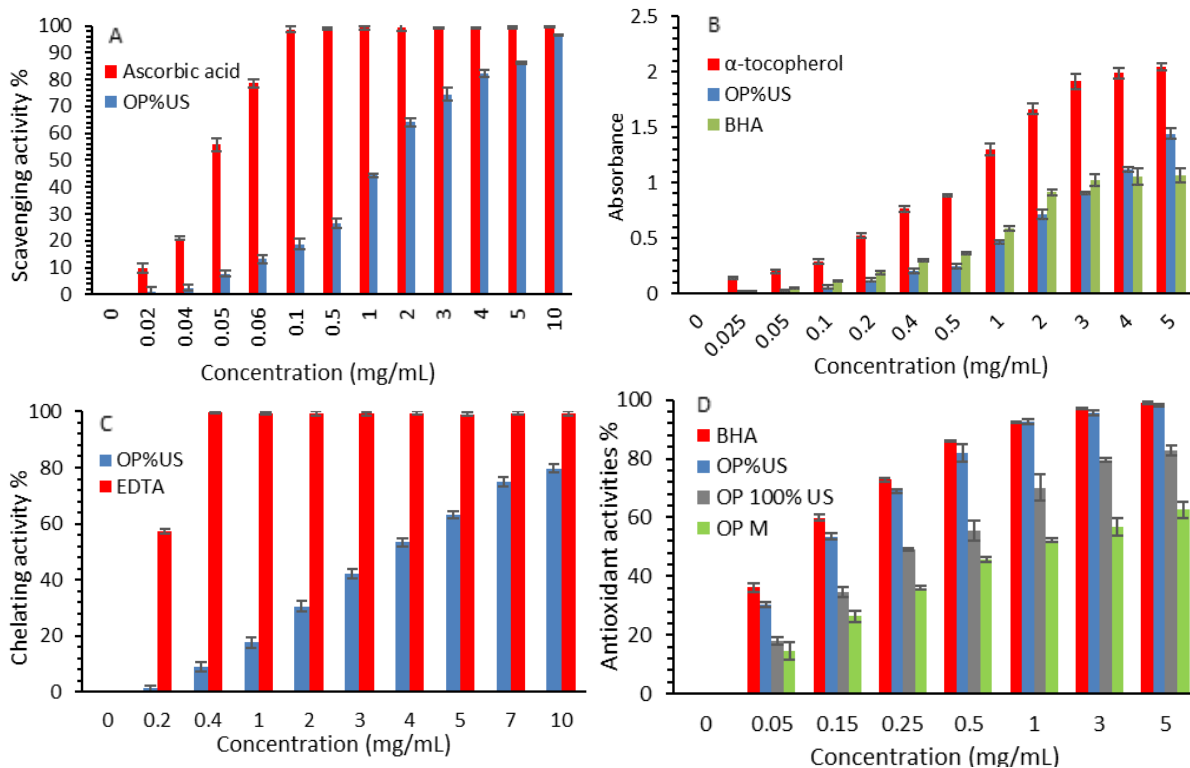


Fig. 4 Antioxidant activity of OP%US against: ABTS radical (A), total antioxidant capacity (B), metal-chelating power (C), β-carotene bleaching (D).

598
 599 The inhibition activity of different polysaccharides on β-carotene bleaching has been studied
 600 by many researchers. Major difference was observed between the reported values. The highest
 601 bleaching inhibition rate (82.3%) was reported by Han *et al.* for polysaccharides from *Plantago*
 602 *depressa* at 3.0 mg/mL [37]. Khatua *et al.* reported a maximum inhibition activity of 53% for
 603 polysaccharides from *Russula senecis Elicits* at 0.5mg/ml, and an IC50 value of 0.49 mg/mL [38].
 604 In contrast, a value of 13.0 % and 19.3% was obtained by Rukiye *et al.* for polysaccharides from
 605 *tragacanth gum* at 20 mg/mL and from locust bean gum at 10 mg/mL, respectively [39]. And Li
 606 *et al.* reported an IC50 of 0.14 mg/mL for polysaccharides from *Lycium barbarum fruits* [40].
 607 Interestingly, in comparison with the literature, the extract obtained in the present work
 608 displays a more efficient antioxidant activity against lipophilic radicals compared to hydrophilic
 609 radicals, suggesting that it could have an anti-cancer activity [34].
 610

611 4 Conclusions

612 Optimization of polysaccharides extraction was carried out for the first time via combination
 613 of two extraction methods, i.e. maceration and ultrasound treatment by using the Surface

614 Response Methodology. Four influencing parameters were considered, namely total extraction
615 time, extraction temperature, ratio of water volume to raw material mass, and time percentage
616 of US treatment in the extraction process.

617 The interaction between parameters and their effects on the extraction yield and
618 polysaccharides yield were investigated. The models to predict the optimal conditions have
619 been validated by additional experiments.

620 The combination of both extraction methods improves the extraction and polysaccharides
621 yields. The combined system allows to significantly reduce the time of extraction, the
622 temperature and volume to mass ratio, and to improve the purity which is of major importance
623 for potential applications. Finally, the optimum extraction process consists of a maximum
624 duration of 20 min maceration and 20 min US treatment at relatively low temperature (ca.
625 44°C) using only water as solvent.

626 The extract is identified as fructo-polysaccharides the RMN analysis indicate that the OP%US
627 possessed a backbone of (2→6)-linked β-d-fructofuranosyl (Fruf), with (2→1)-linked β -d-Fruf
628 branched chains, and terminated with glucose and fructose residues. It presents good
629 antioxidant activities as evidenced by ABTS radical scavenging activity, reducing activity of
630 molybdate, metal-chelating power, and β-carotene bleaching tests. The RSM allowed designing
631 an efficient process to extract polysaccharides from *Ornithogalum billardieri* with remarkable
632 anti-oxidant properties. Additionally, the combined system enhances the anti-lipophilic radical
633 activity of the extract. These natural compounds could be promising as alternative to synthetic
634 antioxidants like BHA for applications in agro-food and pharmaceutical industries.

635 **Conflicts of interest**

636 There are no conflicts of interest to declare.

637 **Acknowledgements**

638 M. K. Medlej benefits of Baalbeck's municipality fellowship. The work was financially supported by Platform for
639 Research and Analysis in Environmental Sciences (Lebanon) and by Institut Européen des Membranes (France).

640 **References**

- 641 [1] V. Labrador, P. Fernández Freire, J.M. Pérez Martín, M.J. Hazen, Cytotoxicity of
642 butylated hydroxyanisole in Vero cells, Cell Biol. Toxicol. 23 (2007) 189–199.
643 <https://doi.org/10.1007/s10565-006-0153-6>.
- 644 [2] J.K. Yan, Y.Y. Wang, H. Le Ma, Z. Bin Wang, Ultrasonic effects on the degradation
645 kinetics, preliminary characterization and antioxidant activities of polysaccharides from

646 *Phellinus linteus* mycelia, *Ultrason. Sonochem.* 29 (2016) 251–257.
647 <https://doi.org/10.1016/j.ultsonch.2015.10.005>.

648 [3] R. Chen, F. Meng, Z. Liu, R. Chen, M. Zhang, Antitumor activities of different fractions of
649 polysaccharide purified from *Ornithogalum caudatum* Ait, *Carbohydr. Polym.* 80 (2010) 845–
650 851. <https://doi.org/10.1016/j.carbpol.2009.12.042>.

651 [4] Z. Persin, K. Stana-Kleinschek, T.J. Foster, J.E.G. Van Dam, C.G. Boeriu, P. Navard,
652 Challenges and opportunities in polysaccharides research and technology: The EPNOE views
653 for the next decade in the areas of materials, food and health care, *Carbohydr. Polym.* 84 (2011)
654 22–32. <https://doi.org/10.1016/j.carbpol.2010.11.044>.

655 [5] A.I. Gray, *Natural Products Isolation*, Second, Humana Press Inc., 2006.

656 [6] Z. Hrom, Ultrasonic extraction of plant materials — investigation of hemicellulose
657 release from buckwheat hulls, *Ultrason. Sonochem.* 10 (2003) 127–133.
658 [https://doi.org/10.1016/S1350-4177\(03\)00094-4](https://doi.org/10.1016/S1350-4177(03)00094-4).

659 [7] Z. Ying, X. Han, J. Li, Ultrasound-assisted extraction of polysaccharides from mulberry
660 leaves, *Food Chem.* 127 (2011) 1273–1279. <https://doi.org/10.1016/j.foodchem.2011.01.083>.

661 [8] Y. Wang, A. Cornea, C. Wang, M. Guo, Effects of Ultrasound Treatment on Extraction
662 and Rheological Properties of Polysaccharides from, *Molecules.* 24 (2019) 939.
663 <https://doi.org/10.3390/molecules24050939>.

664 [9] A. Ebringerová, Z. Hromádková, An overview on the application of ultrasound in
665 extraction, separation and purification of plant polysaccharides, *Cent. Eur. J. Chem.* 8 (2010)
666 243–257. <https://doi.org/10.2478/s11532-010-0006-2>.

667 [10] S. Wang, X. Dong, J. Tong, Optimization of enzyme-assisted extraction of
668 polysaccharides from alfalfa and its antioxidant activity, *Int. J. Biol. Macromol.* (2013) 1–10.
669 <https://doi.org/10.1016/j.ijbiomac.2013.09.029>.

670 [11] M. DuBois, K.A. Gilles, J.K. Hamilton, P.A. Rebers, F. Smith, Colorimetric Method for
671 Determination of Sugars and Related Substances, *Anal. Chem.* 28 (1956) 350–356.
672 <https://doi.org/10.1021/ac60111a017>.

673 [12] D. Tang, S. Yu, Y. Ho, B. Huang, G. Tsai, H. Hsieh, Food Hydrocolloids Characterization of
674 tea catechins-loaded nanoparticles prepared from chitosan and an edible polypeptide, *Food*
675 *Hydrocoll.* 30 (2013) 33–41. <https://doi.org/10.1016/j.foodhyd.2012.04.014>.

676 [13] S.A. Mohamed, J.A. Khan, Antioxidant capacity of chewing stick miswak *Salvadora*
677 *persica*, *Complement. Altern. Med.* 19 (2013) 40. <https://doi.org/10.1186/1472-6882-13-40>.

678 [14] L. Sutharson, P.K. Kar, L.K. Nath, Shila.E.Besra, R.V.S. Joseph, Free radical scavenging
679 activity of leaves of *BISCHOFIA JAVANICA* BLUME AND *FRAXINUS FLORIBUNDA* WALLICH,
680 *Pharmacologyonline.* 1332 (2009) 1324–1332.

- 681 [15] I.I. Koleva, T.A. Van Beek, J.P.H. Linssen, A. De Groot, L.N. Evstatieva, Screening of Plant
682 Extracts for Antioxidant Activity : a Comparative Study on Three Testing Methods, *Phytochem.*
683 *Anal.* 13 (2002) 8–17. <https://doi.org/10.1002/pca.611>.
- 684 [16] A. Raza, F. Li, X. Xu, J. Tang, Optimization of ultrasonic-assisted extraction of antioxidant
685 polysaccharides from the stem of *Trapa quadrispinosa* using response surface methodology,
686 *Int. J. Biol. Macromol.* 94 (2017) 335–344. <https://doi.org/10.1016/j.ijbiomac.2016.10.033>.
- 687 [17] P.F. Jean LEYBROS, Extraction solide-liquide.Aspects théoriques, *Tech. l'ingenieur.* 3
688 (2019) 2–21.
- 689 [18] R. Chen, Y. Li, H. Dong, Z. Liu, S. Li, S. Yang, X. Li, Optimization of ultrasonic extraction
690 process of polysaccharides from *Ornithogalum Caudatum* Ait and evaluation of its biological
691 activities, *Ultrason. Sonochem.* 19 (2012) 1160–1168.
692 <https://doi.org/10.1016/j.ultsonch.2012.03.008>.
- 693 [19] Q. Chen, S.Z. Zhang, H.Z. Ying, X.Y. Dai, X.X. Li, C.H. Yu, H.C. Ye, Chemical characterization
694 and immunostimulatory effects of a polysaccharide from *Polygoni Multiflori Radix Praeparata*
695 in cyclophosphamide-induced anemic mice, *Carbohydr. Polym.* 88 (2012) 1476–1482.
696 <https://doi.org/10.1016/j.carbpol.2012.02.055>.
- 697 [20] X. Wang, R. Sun, J. Zhang, Y. Chen, N. Liu, Structure and antioxidant activity of
698 polysaccharide POJ-U1a extracted by ultrasound from *Ophiopogon japonicus*, *Fitoterapia.* 83
699 (2012) 1576–1584. <https://doi.org/10.1016/j.fitote.2012.09.005>.
- 700 [21] K. Zhong, Q. Zhang, L. Tong, L. Liu, X. Zhou, S. Zhou, Molecular weight degradation and
701 rheological properties of schizophyllan under ultrasonic treatment, *Ultrason. Sonochem.* 23
702 (2015) 75–80. <https://doi.org/10.1016/j.ultsonch.2014.09.008>.
- 703 [22] G.L. Ailiesei, M. Ciobanu, M. Balan, C. Stavarache, L. Barbes, A. Nicolescu, C. Deleanu,
704 NMR detected metabolites in complex natural fluids. Quinic acid in apple juice, *Ovidius Univ.*
705 *Ann. Chem.* 26 (2015) 51–56. <https://doi.org/10.2478/auoc-2015-0009>.
- 706 [23] J. Liu, A.L. Waterhouse, N.J. Chatterton, Proton and carbon NMR chemical-shift
707 assignments for [β -d-Fruf-(2 \rightarrow 1)]₃-(2 \leftrightarrow 1)- α -d-Glcp (nystose) and [β -d-Fruf-(2 \rightarrow 1)]₄-(2 \leftrightarrow
708 1)- α -d-Glcp (1,1,1-kestopentaose) from two-dimensional NMR spectral measurements,
709 *Carbohydr. Res.* 245 (1993) 11–19. [https://doi.org/10.1016/0008-6215\(93\)80056-K](https://doi.org/10.1016/0008-6215(93)80056-K).
- 710 [24] C. Wang, D. Hua, C. Yan, Structural characterization and antioxidant activities of a novel
711 fructan from *Achyranthes bidentata* Blume, a famous medicinal plant in China, *Ind. Crops Prod.*
712 70 (2015) 427–434. <https://doi.org/10.1016/j.indcrop.2015.03.051>.
- 713 [25] L. Zhang, N. Reddy, C. Soo Khoo, S. Rao Koyyalamudi, C.E. Jones, Antioxidant and
714 Immunomodulatory Activities and Structural Characterization of Polysaccharides Isolated from

715 *Lobelia chinensis* Lour, *Pharmacologia*. 9 (2018) 157–168.
716 <https://doi.org/10.5567/pharmacologia.2018.157.168>.

717 [26] J. Chen, K.L. Cheong, Z. Song, Y. Shi, X. Huang, Structure and protective effect on UVB-
718 induced keratinocyte damage of fructan from white garlic, *Carbohydr. Polym.* 92 (2013) 200–
719 205. <https://doi.org/10.1016/j.carbpol.2012.09.068>.

720 [27] A. Luo, X. He, S. Zhou, Y. Fan, A. Luo, Z. Chun, Purification , composition analysis and
721 antioxidant activity of the polysaccharides from *Dendrobium nobile* Lindl ., *Carbohydr. Polym.*
722 79 (2010) 1014–1019. <https://doi.org/10.1016/j.carbpol.2009.10.033>.

723 [28] L. Cell, Characterization and Antioxidant Activities of Yellow Strain *Flammulina velutipes*
724 (Jinhua Mushroom) Polysaccharides and Their E ff ects on ROS Content in, *Antioxidants*. 8
725 (2019) 1–15. <https://doi.org/10.3390/antiox8080298>.

726 [29] William Pratt, Transformation of Glucocorticoid and Progesterone Receptors to the
727 DNA-Binding State, *J. Cell. Biochem.* 68 (1987) 51–68.

728 [30] K. Pavithra, S. Vadivukkarasi, Evaluation of free radical scavenging activity of various
729 extracts of leaves from *Kedrostis foetidissima* (Jacq .) Cogn ., *Food Sci. Hum. Wellness*. 4 (2015)
730 42–46. <https://doi.org/10.1016/j.fshw.2015.02.001>.

731 [31] L.S. Costa, L.T.D.B. Nobre, G.P. Fidelis, S.L. Cordeiro, R.M. Oliveira, D.A. Sabry, R.B.G. Ca,
732 M.S.S.P. Costa, E.H.C. Farias, E.L. Leite, H.A.O. Rocha, Biological activities of sulfated
733 polysaccharides from tropical seaweeds, *Biomed. Pharmacother.* 64 (2010) 21–28.
734 <https://doi.org/10.1016/j.biopha.2009.03.005>.

735 [32] H. Qi, Q. Zhang, T. Zhao, R. Chen, Q. Huimin, Z. Quanbin, Z. Tingting, C. Rong, Gz. Hon,
736 N. Xizhen, L. Zhien, Antioxidant activity of different sulfate content derivatives of
737 polysaccharide extracted from *Ulva pertusa* (Chlorophyta) in vitro, *Int. J. Biol. Macromol.* 37
738 (2005) 195–199. <https://doi.org/10.1016/j.ijbiomac.2005.10.008>.

739 [33] L. Unten, M. Koketsu, M. Kim, Antidiscoloring Activity of Green Tea Polyphenols on -
740 Carotene, *J. Agric. Food Chem.* 8561 (2012) 1–3.

741 [34] G. Amandine, *Plantes médicinales et antioxydants*, TOULOUSE III PAUL SABATIER, 2016.

742 [35] X. Guo, X. Shang, X. Zhou, B. Zhao, J. Zhang, Ultrasound-assisted extraction of
743 polysaccharides from *Rhododendron aganniphum*: Antioxidant activity and rheological
744 properties, *Ultrason. Sonochem.* 38 (2017) 246–255.
745 <https://doi.org/10.1016/j.ultsonch.2017.03.021>.

746 [36] W. Tang, L. Lin, J. Xie, Z. Wang, H. Wang, Y. Dong, M. Shen, M. Xie, Effect of ultrasonic
747 treatment on the physicochemical properties and antioxidant activities of polysaccharide from
748 *Cyclocarya paliurus*, *Carbohydr. Polym.* 151 (2016) 305–312.
749 <https://doi.org/10.1016/j.carbpol.2016.05.078>.

- 750 [37] N. Han, L. Wang, Z. Song, J. Lin, C. Ye, Z. Liu, J. Yin, International Journal of Biological
751 Macromolecules Optimization and antioxidant activity of polysaccharides from *Plantago*
752 *depressa*, Int. J. Biol. Macromol. 93 (2016) 644–654.
753 <https://doi.org/10.1016/j.ijbiomac.2016.09.028>.
- 754 [38] S. Khatua, K. Acharya, Water Soluble Antioxidative Crude Polysaccharide From *Russula*
755 *senecis* Elicits TLR Modulated NF- κ B Signaling Pathway and Pro-inflammatory Response in
756 Murine Macrophages, Front. Pharmacol. 9 (2018) 1–11.
757 <https://doi.org/10.3389/fphar.2018.00985>.
- 758 [39] R. Boran, A. Ugur, N. Sarac, Investigation of Hyaluronidase, Collagenase and Elastase
759 Inhibitory Potentials and Comparative Evaluation of the Antimicrobial, Antioxidant and
760 Homeostatic Activities of Two Natural Polysaccharides, J. Nat. Appl. Sci. 22 (2018) 1182–1189.
761 <https://doi.org/10.19113/sdufenbed.471994>.
- 762 [40] X.M. Li, X.L. Li, A.G. Zhou, POLYMER Evaluation of antioxidant activity of the
763 polysaccharides extracted from *Lycium barbarum* fruits in vitro, Eur. Polym. J. 43 (2007) 488–
764 497. <https://doi.org/10.1016/j.eurpolymj.2006.10.025>.
- 765